Stability improvement of Rh/γ-Al_2O_3 catalyst layer by ceria doping for steam reforming in an integrated catalytic membrane reactor system

Sreekumar Kurungot and Takeo Yamaguchi*

Department of Chemical System Engineering, The University of Tokyo, 7-3-1 Hongo, Bunkyo-ku, Tokyo-113, Japan

Received 5 August 2003; accepted 17 November 2003

Significant improvement over the equilibrium methane conversion level was achieved by performing the reforming of methane in a catalytic membrane reactor, which was prepared by integrating a microporous silica membrane with a sandwiched-type Rh/γ-Al_2O_3 catalyst layer. However, the methane conversion activity decreased progressively owing to the deactivation of the intermediate catalyst layer under the reaction environments. On the other hand, addition of CeO_2 as a promoter for the Rh/γ-Al_2O_3 catalyst significantly improved the catalyst stability. The improvement was achieved probably by the kinetic and oxidative stabilization of the catalyst matrix with CeO_2. However, compared to the nonpromoted system, the ceria-promoted systems displayed lower catalytic activities based on the Rh/Ce ratios. The results led to the conclusion that a controlled interplay of the catalytic potentiality of Rh and the stabilization effect of Ce are essential to obtain an acceptable system. The membrane quality and its performance decreased especially with high Ce incorporation in the catalyst layer, possibly as a result of the observed microstructural variations in the catalyst layer with the Ce addition. Therefore, a consensus between the activity and stability of the material as a catalyst and the textural characteristics of the catalyst layer as a support layer for the silica membrane is considered to be an important factor that decides the success of the approach. A possible mechanism has been suggested to explain the role of ceria as a promoter in the Rh/γ-Al_2O_3 system.

KEY WORDS: inorganic membrane; membrane reactor; steam reforming; silica membrane; promoter.

1. Introduction

In a recent paper, the authors have reported about a compact catalytic membrane reactor system possessing a Rh/γ-Al_2O_3 catalytic layer integrated with a sol–gel synthesized microporous silica membrane [1]. The important structural feature of the system was a "sandwiched"-type catalytic layer, which was placed in between the layer of a hydrogen perm-selective silica membrane on the upper side and the surface of an α-Al_2O_3 support tube on the inner side. By making such a direct combination of a membrane-catalyst assembly, unlike the combination of a packed catalyst bed and a membrane, good improvement over the rate of mass transfer and heat exchange along the interfaces can be achieved. We have reported that the system was exhibiting improved efficiency in the reforming of CH_4 at comparatively lower operating temperatures and steam-to-C molar ratios than the conventional fixed-bed reforming systems. For example, under optimized conditions, a nearly 25–30% improvement from the equilibrium conversion level was achieved as a result of abstraction of hydrogen from the product stream by the silica membrane integrated with the catalyst layer. However, unfortunately, the extent of improvement from the equilibrium value steadily decreased after a few hours of nearly stable performance. The change in the permeation properties of the silica membrane, under prolonged exposure to the reaction conditions, was rather small compared to the large deactivation rate. Therefore, we presumed that a major cause of efficiency drop was as a result of deactivation of the Rh/γ-Al_2O_3 catalyst layer, possibly by the deposition of carbonaceous products or by textural variations such as particle agglomeration and, thereby, causing progressive reduction in the number of available active sites for the reaction. In order to address the activity drop and to stabilize the system, we have performed a series of experiments. A study using promoters for the Rh/γ-Al_2O_3 catalyst was found to be very promising, and, therefore, in the present paper, we highlight the important findings of this study.

In the case of Rh supported on Al_2O_3, the CH_4 adsorption rate decreases significantly owing to removal of oxygen from the catalyst [2–3]. However, addition of small amounts of air along with steam during reforming can replenish the oxygen loss due to the high adsorption rate of oxygen on Rh [4]. Alternatively, the oxygen-binding capacity of the Rh/γ-Al_2O_3 system can be improved by incorporating certain oxygen transporting additives such as CeO_2 [5–7]. In addition to its ability to

* To whom correspondence should be addressed.
E-mail: yamag@chemsys.t.u-tokyo.ac.jp

1011-372X/04/0200–0181/0 © 2004 Plenum Publishing Corporation

store and release oxygen, CeO_2 stabilizes support alumina and improves the dispersion state of precious metals [8–11]. Therefore, we have employed CeO_2 as a promoter for the $Rh/\gamma\text{-}Al_2O_3$ system and the performance was evaluated for reforming studies. The performance evaluation result of the nonpromoted system (i.e. $Rh/\gamma\text{-}Al_2O_3$ system) is also discussed briefly to make the comparison more clear and meaningful.

2. Experimental

2.1. Preparation of catalytic membrane

Boehmite (γ-AlOOH) sol was prepared by using the standard recipe reported elsewhere [12]. The Ce-Rh/\gamma-Al_2O_3 systems with different Rh/Ce wt.% ratios like 1/0, 1/0.5, 1/1 and 1/2 were prepared by incorporating stoichiometric amounts of the components in the boehmite sol. A solution of polyvinyl alcohol (1 wt.%) with $RhCl_3 \cdot 2H_2O$ and/or $Ce(NO_3)_3 \cdot 6H_2O$, based on the Rh/Ce ratio, was added to the boehmite sol and the sol concentration was adjusted either by evaporation or by dilution with deionized water. The sol was used for dip-coating the outer surface of an $\alpha\text{-}Al_2O_3$ tube (pore size $\sim 0.1\mu$m; length 3.5 cm; top part sealed), which was fixed on a dense ceramic tube by glass sealing. The dip-coated layer was dried at 50°C and calcined at 600°C at a heating and cooling rate of 25 °Ch^{-1}. The whole procedure was repeated twice to obtain a crack-free layer of $Ce\text{-}Rh/\gamma\text{-}Al_2O_3$. Silica sol was prepared by acid hydrolysis (HNO_3, 1 mol l^{-1} solution) and condensation of tetrahydroorthosilicate (TEOS) in ethanol as reported by Nair *et al.* [13]. HNO_3 was added slowly to a mixture of known quantities of ethanol (Wako Pure Chemical Industries) and TEOS (Aldrich Chemical) with gentle stirring. After keeping the mixture at RT for about 30 min, the temperature was raised slowly to 70 °C and the mixture was refluxed at this temperature for 3 h to obtain the sol of the desired quality. The final dipping solution was prepared by diluting the silica sol to a concentration of 0.1 molL^{-1} using ethanol. The $\alpha\text{-}Al_2O_3$ tube, with the $Ce\text{-}Rh/\gamma\text{-}Al_2O_3$ surface was dipped into the silica sol (dipping time 10 s) and dried at 40 °C in a humidity-controlled oven with 60% RH. The sample was calcined at 600 °C in a temperature-controlled furnace to obtain a thin layer of silica over the catalyst layer. A nonpromoted system (i.e. $Rh/\gamma\text{-}Al_2O_3$) was also prepared in a similar way for the purpose of comparison. The designations and compositions of the prepared catalytic membranes are summarized in table 1.

2.2. Membrane reactor

A detailed discussion about the membrane reactor setup was given in the previous paper [1]. Both the gas-permeation studies and reforming experiments can be performed using the same setup, and pressure sensors and on-line gas chromatograph respectively were used to measure the permeation values and CH_4 conversions. Permeation values were standardized with units of mol m^{-2} s^{-1} Pa^{-1}. A sweep gas flow was maintained on the permeate side during the reforming experiments. Both the permeate and retentate fluxes were separately analyzed using the on-line GC fitted with an active carbon column and a thermal conductivity detector to measure the total CH_4 conversion.

3. Results and discussion

3.1. Physical characteristics

TEM (JEOL Hightech Co. Ltd.) analysis of a cross section of CRAL-0.5 revealed the interface of the silica membrane and the $Rh\text{-}Ce/\gamma\text{-}Al_2O_3$ catalyst layer. The silica membrane was continuous and possessed a thickness of $\sim$50nm throughout the length of the cross section. Figure 1 shows the TEM image of the cross section of the $Rh\text{-}Ce/\gamma\text{-}Al_2O_3$ catalyst layer and the $\alpha\text{-}Al_2O_3$ support surface. Irrespective of the fact that the support tube possesses a pore size of $\sim$ 0.1 μm, the penetration of the catalyst particles into the pores of the $\alpha\text{-}Al_2O_3$ support tube was negligible or it was only a few nanometers from the interface region, as was evident by the predominance of empty pores in the interface as that in the bulk of the support material. Therefore, the effective reaction zone can be fairly considered as the area of the catalytic layer between the membrane and the support. Except CRAL-2, all other membranes showed similar continuous and crack-free silica and catalyst layers. In the case of CRAL-2, however, the catalyst layer was weakly adhered to the support, as was evident from the FESEM image in figure

Table 1
Composition of the catalyst layer and the surface area, pore diameter and pore-volume data

Membrane designation	Catalyst layer composition (wt%)	Surface area (BET), m^{2}g^{-1}	Pore diameter (BJH_D)[a], nm	Pore volume[b] cm^3/g
AL	$\gamma\text{-}Al_2O_3$	272.9	4.1	0.33
RAL	Rh (1%)/$\gamma\text{-}Al_2O_3$	284.3	4.3	0.36
CRAL-0.5	Ce (0.5%)Rh(1%)/$\gamma\text{-}Al_2O_3$	197.7	5.3	0.32
CRAL-1.0	Ce (1.0%)Rh(1%)/$\gamma\text{-}Al_2O_3$	197.3	5.5	0.33
CRAL-2.0	Ce (2.0%)Rh(1%)/$\gamma\text{-}Al_2O_3$	–	–	

[a] BJH: Barette–Jovner–Halenda; the subscript D indicates desorption.
[b] BJH cumulative pore volume of pores between 1.7 and 300 nm diameter.

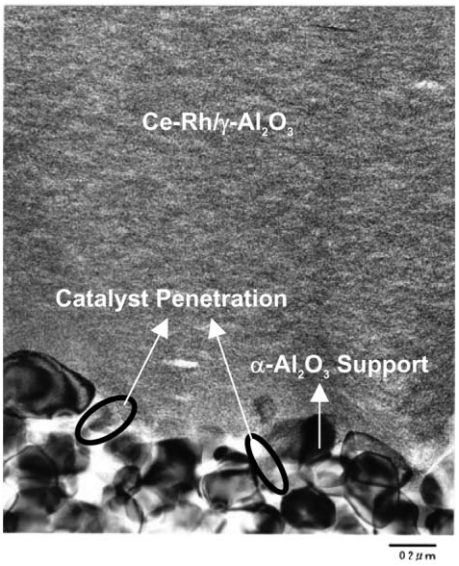

Figure 1. The TEM imageof the (Ce-Rh)/γ-Al_2O_3-α-Al_2O_3 interface.

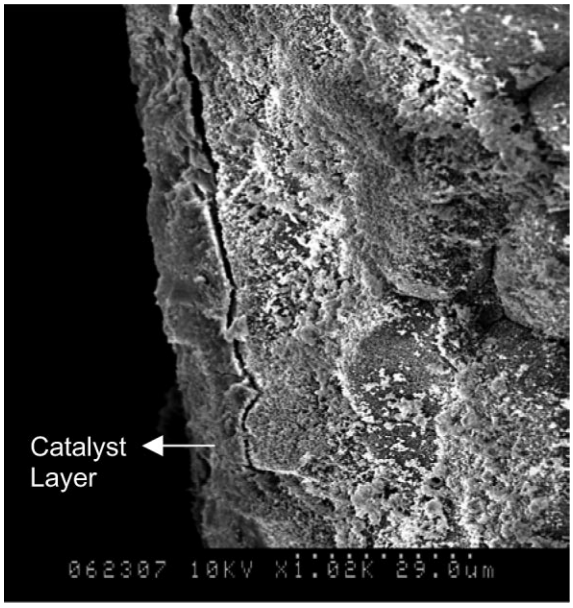

Figure 2. The FESEM image showing the partially detached Ce-Rh/γ-Al_2O_3 catalytic layer, which contains 2 wt.% of Ce as a promoter. The specimen was analyzed before the surface of the catalyst layer was coated with the silica membrane.

2. The figure shows a partially detached layer of the catalyst (the image was obtained by scanning the cross section with a Hitachi S-900 FESEM instrument). In fact, the detrimental effect of increased ceria loading on the mechanical stability of the catalyst layer created a limitation in the choice of a range of CeO_2-promoted systems with different Rh/Ce ratios. In other words, the consensus between the activity (and stability) of the material as a catalyst and the mechanical stability of the catalyst layer as a support layer for the silica membrane is an important factor, and, as a result of this, a minimum required promoter concentration to stabilize the catalyst material had to be preferred. On the basis of the above results, we restricted the detailed reforming experiments only to the systems possessing Ce concentration of ≤ 1.0 wt.%.

The XRD patterns CRAL-1.0 and RAL were obtained by scanning the respective powdered catalyst samples using a Philips PW 1710 X-ray diffractometer. Characteristic XRD peaks of Rh_2O_3 (114) and (110) planes at 2θ values of 33° and 36° were observed in the case of both RAL and CRAL-1.0. The calculated particle size of Rh_2O_3, based on Scherrer's equation, was 4.4 nm. The XRD pattern of CRAL-1.0 did not reveal any clear diffraction peaks of CeO_2. Basically, the diffraction pattern of CRAL-1.0 was identical to that of RAL. Probably, CeO_2 is in an amorphous state or the particles are very well dispersed in the alumina phase, with the crystalline phases being hardly detected during the scanning.

The BET surface area and pore diameter data of the respective powdered catalyst samples were obtained by the N_2 sorption method using Micromeritics surface area analyzer. The data are summarized in table 1. Both γ-Al_2O_3 (AL) and its Rh incorporated from RAL-1.0 displayed very close surface area and pore diameter values and, based on the results, it can be concluded that the Rh particles are dispersed in the γ-Al_2O_3 matrix without obviously changing the microstructure of the latter. However, a drop in the surface area value with Ce-doping was noticed, as is evident from table 1, for both CRAL-0.5 and CRAL-1.0. A comparison graph as shown in figure 3 would be helpful in elucidating the changes of the pore-structure characteristics as a function of composition. The increase in pore-volume and pore-diameter values after Rh incorporation, i.e., for RAL-1.0, was small or negligible, whereas Ce-addition resulted in noticeable increase in the pore-diameter values with some expanse in the pore-volume value originally possessed by AL. Such variations in the microstructure of the parent γ-Al_2O_3 matrix due to Ce-addition can detrimentally affect the quality and performance of the upper lying silica membrane if the variations exceed by a few nanometers. These results along with the outcomes of the previously discussed TEM/FESEM observations restricted us from using the CeO_2 concentration beyond a certain limit.

3.2. Permeation properties

Table 2 comprises the permeation data of the catalytic membranes in the temperature range of 100–525 °C using H_2 or CH_4 as the feed gas. In all cases, H_2, with a kinetic diameter of 2.8 Å, showed activated transport throughout the temperature range of 100–525 °C. However, in the case of CH_4, which

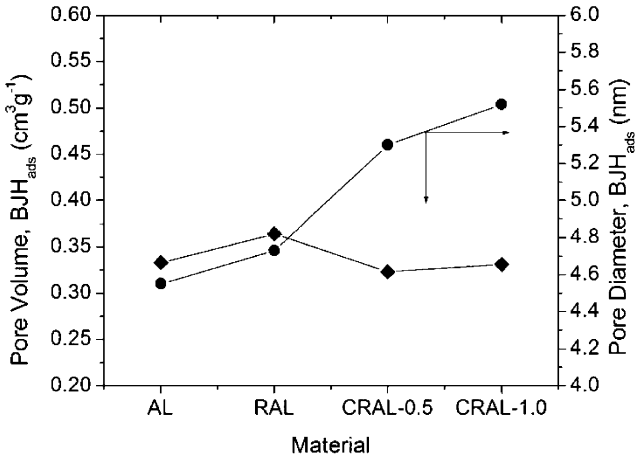

Figure 3. Variation of pore volume and pore diameter with addition of Rh and Ce in the γ-Al_2O_3 matrix.

possesses a kinetic diameter of 3.7 Å, the gas transport was nearly Knudsen type. These results clarify the microporous nature of the silica layer, with a majority of its pores having dimensions <3.7 Å. As a net effect of the differences in the permeation properties of H_2 and CH_4, the separation factor for H_2 to CH_4 increased with increase in temperature. For example, in the case of RAL, the separation factor for H_2/CH_4, which was nearly 7.5 at 100 °C, increased progressively with increase in temperature and was ~31 at 525 °C. In this case, the hydrogen permeation was activated with an apparent activation energy of 6.8 kJ/mol. However, in the case of the Ce-incorporated membranes viz. CRAL-0.5 and CRAL-1.0, even though the general permeation characteristics for both H_2 and CH_4 resemble those over RAL, both these membranes displayed slightly lower H_2 to CH_4 separation factors. Those textural variations during Ce incorporation, as detailed under Section 3.1, have possibly influenced the quality of the silica membrane and thereby resulted in some drop in the separation factor values.

3.3. Reforming of methane

A detailed discussion about the activity evaluation and process optimization studies for the catalytic membrane possessing a nonpromoted $Rh/\gamma\text{-}Al_2O_3$ catalyst layer (i.e. the system RAL, as designated in this paper) was made in the previous paper [1]. The optimized conditions were as follows: reaction temperature 525 °C; steam-to-C molar ratio 3.5; and contact time 0.015 gscm^{-3}. The present discussion is mainly focused on exploring the influencing role of ceria as a promoter to impart catalyst stability under the reforming environments. Therefore, the catalytic activity trend

Table 2
Gas transport data for H_2 and CH_4 over the different catalytic membranes prepared

Membrane designation	Temperature °C	Permeation (mol.m^{-2}.s^{-1}.Pa)		Separation factor H_2/CH_4
		H_2	CH_4	
RAL	100	9.28×10^{-8}	1.24×10^{-8}	7.5
	200	1.54×10^{-7}	1.14×10^{-8}	13.5
	300	1.94×10^{-7}	1.10×10^{-8}	17.6
	400	2.35×10^{-7}	1.09×10^{-8}	21.6
	500	2.85×10^{-7}	1.05×10^{-8}	27.1
	525	3.01×10^{-7}	0.96×10^{-8}	31.4
CRAL-0.5	100	1.55×10^{-7}	1.14×10^{-8}	13.6
	200	1.94×10^{-7}	1.10×10^{-8}	17.6
	300	2.35×10^{-7}	1.10×10^{-8}	21.4
	400	2.65×10^{-7}	1.07×10^{-8}	24.8
	500	2.86×10^{-7}	1.07×10^{-8}	26.7
	525	2.87×10^{-7}	1.06×10^{-8}	27.1
CRAL-1.0	100	9.79×10^{-8}	9.65×10^{-9}	10.2
	200	1.43×10^{-7}	9.10×10^{-9}	15.7
	300	1.80×10^{-7}	9.20×10^{-9}	19.6
	400	2.13×10^{-7}	9.20×10^{-9}	23.2
	500	2.21×10^{-7}	9.21×10^{-9}	24.0
	525	2.23×10^{-7}	9.21×10^{-9}	24.2

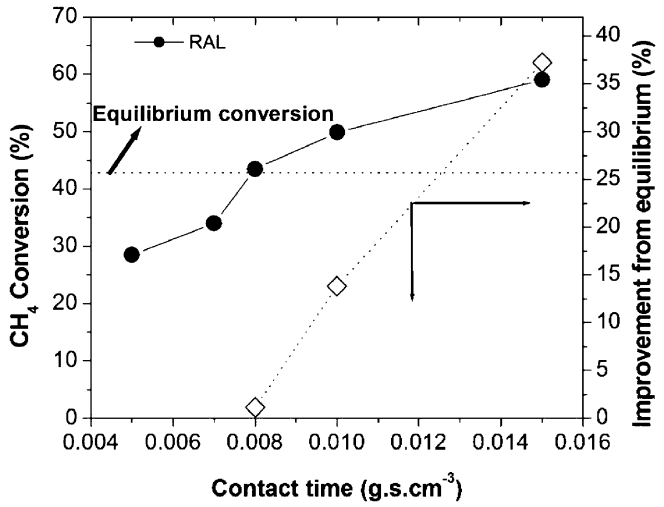

Figure 4. Effect of contact time on methane conversion and improvement over the equilibrium level using the catalytic membrane RAL. (Reaction temperature = 525°C; H_2O/C molar ratio = 3.5).

and stability concerns of RAL are discussed briefly at first and thereafter a discussion about the performance of the Ce-promoted systems is given. A discussion about a plausible mechanism concerning the stabilization effect of ceria has also been mentioned in the latter part of the paper.

CH_4, diluted with Ar and air to a volume of 30% and O/C (where 'C' represents carbon in CH_4) molar ratio of 1.0, was supplied along with steam to perform the reforming reaction at atmospheric pressure. An N_2 sweep in the rate of 30 cm^3 min^{-1} was maintained in the permeate side to facilitate H_2 transfer. The reaction was performed at 525 °C and the H_2O/C molar ratio was maintained at 3.5. Generally, a mass balance in the range 92–94% was measured during the experiments.

Figure 4 illustrates the CH_4 conversion as a function of contact time (i.e. the time of contact of the reactant mixture per gram of $Rh/\gamma\text{-}Al_2O_3$ catalyst) over the catalytic membrane RAL. The effect of H_2 removal on conversion is demonstrated more explicitly in the same figure by plot of improvement over the equilibrium level for the catalytic membrane. The improved performance of the catalytic membrane can be seen at regions of high contact times, where the conversions obtained were considerably higher than the equilibrium level. CH_4 conversion, which was very close to the equilibrium conversion level of 43% at a contact time of 0.008 $gscm^{-3}$, registered a value of 50% at a contact time of 0.01 $gscm^{-3}$ with a net improvement of more than 16 % from the equilibrium value. The conversion reached nearly 59.5 % at a contact time of 0.015 $gscm^{-3}$, giving a net improvement from the equilibrium level by 37%. However, with further increase in contact time, we observed a color change of the catalytic membrane from light yellow to gray, probably due to carbon deposition into the micropores as a result of the increased rate of CH_4 decomposition as a side reaction at a very high contact time. When the contact time was ≤ 0.007 $gscm^{-3}$, there was no improvement from the equilibrium level. Therefore, the system can be operated effectively in the contact time region of 0.008–0.015 $gscm^{-3}$.

However, even though appreciable CH_4 conversion was achieved over the system RAL under optimized conditions, an important drawback was the vulnerability of the system for deactivation with time of exposure in the reaction environments. It is well documented that the major cause of deactivation in various reforming reactions primarily originates from coke deposition over the catalyst surface and, thereby, affects the direct interaction of the reactants with the active reactive sites. In addition to coke deposition, other reasons like change of oxidation states of the catalytically active components, sintering or aggregation of particles can also result in catalyst deactivation. There are sufficient reports about the promoting influence of CeO_2, especially for noble metal systems, and this quality was recognized as the unique property of ceria to affect (i) the thermal and structural stability of the catalyst carriers, (ii) the dispersion of the supported metal, (iii) the oxidative stabilization of noble metals, (iv) the oxygen storage and release capacities and (v) the decrease of carbon formation on the catalyst surface, etc. [5–11].

The performances of CRAL-0.5, CRAL-1.0 and RAL for conversion of CH_4 as a function of time onstream were evaluated. In the case of RAL, the deactivation was quite rapid especially after the initial few hours of nearly stable performance. However, unlike RAL, which does not contain ceria, the ceria-promoted systems viz. CRAL-0.5 and CRAL-1.0 displayed improved catalyst stability during the reaction. The activity of the system had strong dependence on the Rh/Ce ratios, irrespective of the fact that all the

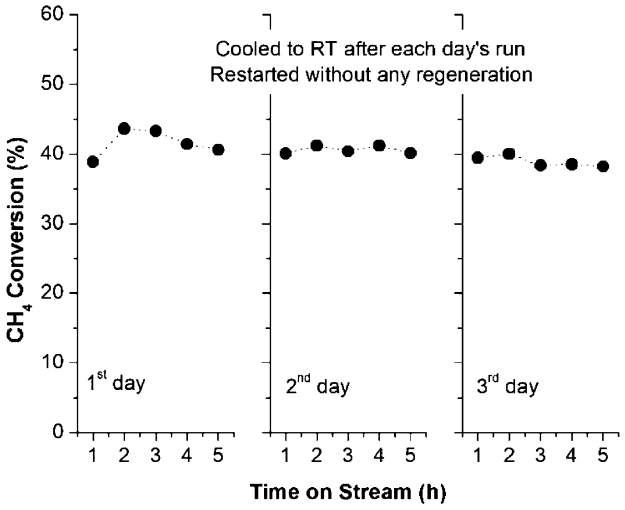

Figure 5. Long-term stability test of CRAL-0.5 for steam reforming of methane. After each day's experiment, the system was cooled to room temperature and restarted on the next day without any regeneration. (Reaction temperature = 525 °C; H_2O/C molar ratio = 3.5).

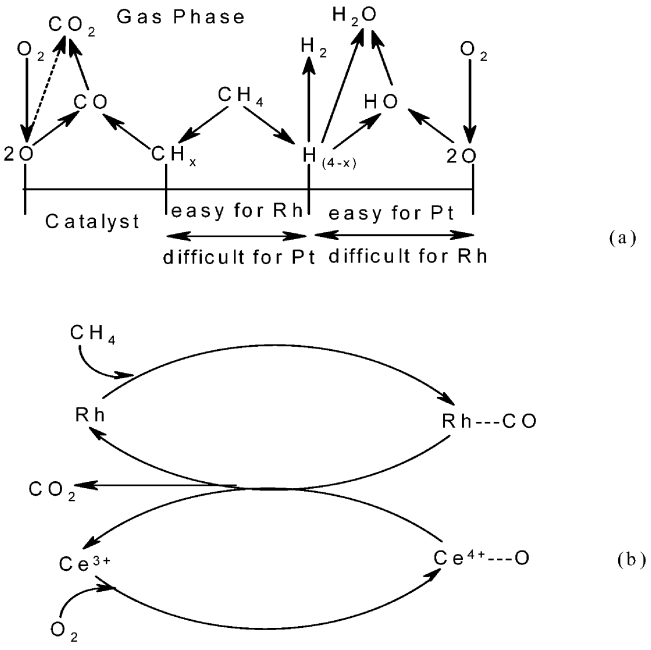

Figure 6 (a) The plausible routes of dissociative adsorption of CH_4 and the consequent reactions. (b) A scheme illustrating how ceria assists the oxygen transport through the system.

promoted systems were more or less equally stable. This could probably be due to the differences in the potentialities of Rh and Ce toward the reaction. The replacement of Ce for Rh or partial coverage of Rh_2O_3 particles by CeO_2 must result in a corresponding drop in the net activity of the system. Still, another probable reason could be the comparatively low surface areas of the promoted systems than that of RAL. On the basis of the results, it can be ascertained that a controlled interplay of the catalytic potentiality of Rh and the stabilization power of Ce must be the critical parameter, and both these factors have to be properly balanced for further improvement of the system. Research in this direction is currently in progress in our laboratory. In addition to the short-term stability test as discussed above, a long-term stability test was performed over the catalytic membrane CRAL-0.5; the result is presented in figure 5. The reaction was continued for several hours each day and cooled to room temperature after each day's run, and the experiment was restarted without any regeneration, as shown in the figure. A fairly continuous plot throughout indicates a comparatively coke-free operation during the time period investigated.

The mechanistic aspects of the promotional influence of ceria on Rh catalysts can be envisaged on the basis of the profound partial oxidation property of the Rh system [2,14]. This along with its strong methane adsorption tendency [2] cause initial formation of CO and H_2. Therefore, at a stoichiometric feed ratio the dominant reaction pathway can be the direct formation of CO and H_2, followed by the consecutive oxidation of CO (consecutive oxidation of H_2 over Rh system is less favorable owing to the comparatively higher activation energy (20 kcal/mol) for Rh, than that for Pt (2.5 kcal/mol)). A plausible route of formation of various products, followed by the dissociative adsorption of CH_4, as suggested by Freni and coworkers [15], is shown in figure 6(a). CO can be formed from surface carbon and oxygen present as rhodium oxide, while the consecutive oxidation of CO proceeds via both chemisorbed oxygen and rhodium oxide. Thus a Mars-van Krevelen redox cycle can be postulated, wherein the adsorbed methane reduces the metal oxide, which gets reoxidized by the oxygen from the feed. The rate of CH_4 adsorption will be significantly reduced unless the oxygen loss is replenished in the process. Ceria, if present in small amounts, can accelerate the oxygen transport property of the system due to its ability to store and release oxygen. This property of ceria is due to the fact that both Ce^{3+} and Ce^{4+} are stable, allowing the oxide to shift between CeO_2 and CeO_{2-x} [16]. The lattice oxygen released during ceria reduction can react with CH_4 and CO under rich conditions. The redox cycle assisted by the oxygen-buffering effect of ceria is represented in figure 6(b).

4. Conclusion

A catalytic membrane reactor system prepared by integrating microporous silica membrane with a sandwiched-type $Rh/\gamma\text{-}Al_2O_3$ catalyst layer can give better efficiency for reforming of CH_4, but due to catalyst deactivation, the extent of improvement decreased progressively with time. Promoting the $Rh/\gamma\text{-}Al_2O_3$ matrix with ceria resulted in significant improvement in the catalyst stability, possibly due to the kinetic and

oxidative stabilization of the catalyst matrix with ceria. However, ceria doping was associated with a concomitant decrease in the activity of the catalyst layer. This, in other words, means that the Ce/Rh ratio has to be carefully optimized considering the promotional influence of ceria, the catalytic potentiality of $Rh/\gamma\text{-}Al_2O_3$ and the microstructural characteristics of the catalyst layer, which is acting as the support for the silica membrane. The outcome of the present study provided valuable contribution in the direction of achieving compact and economically attractive systems and processes in chemical industries.

Acknowledgment

We gratefully acknowledge NEDO for financial support and Dr. B.N. Nair of the Noritake Company Ltd. for fruitful discussions.

References

[1] S. Kurungot, T. Yamaguchi and S.I. Nakao, Catal. Lett. 86(4) (2003) 273.
[2] D. Wang, O. Dewaele and G.F. Froment, J. Mol. Catal., A 136 (1998) 301.
[3] D.A. Hickman and L.D. Schmidt, AIChE J. 39 (1993) 1164.
[4] D.F. Padowitz and S.J. Sibener, Surf. Sci. 254 (1991) 125.
[5] S. Imamura, T. Yamashita, R. Hamada, Y. Saito, Y. Nakao, N. Tsuda and C. Kaito, J. Mol. Catal., A 129 (1998) 249–256.
[6] E.E. Lowenthal, L.F. Allard, M.T. Henry and H.C. Foley, J. Mol. Catal., A 100 (1995) 129–145.
[7] R. Cracium, W. Daniell and H. Knozinger, Appl. Catal., A (in press).
[8] B. Harrison, A.F. Diwell and C. Hallett, Plat. Mat. Rev. 32 (1988) 73.
[9] M. Ozawa and M. Kimura, J. Mater. Sci. Lett. 9 (1990) 291.
[10] A. Cook, A.G. Fitzgerald and J.A. Cairns, in *Catalysis and Surface Characterization*, T.J. Denes, C.H. Rochester and J. Thomson (eds) (Royal Society of Chemistry, Cambridge, 1992) p. 249.
[11] F.L. Normand, L. Hilaire, K. Kili and G. Maire, J. Phy. Chem. 92 (1988) 2561.
[12] B.J.R. Uhhorn, K. Keizer and A.J. Burggrasf, J. Membr. Sci. 66 (1992) 259.
[13] B.N. Nair, K. Keizer, W.J. Elferink, M.J. Gilde, H. Verweij and A.J. Burggraaf, J. Membr. Sci. 116 (1996) 161.
[14] K.H. Hofstad, J.H.B.J. Hoebink, A. Holmen and G.B. Marin, Catal. Today 40 (1998) 157–170.
[15] S. Freni, G. Calogero and S. Cavallaro, J. Power Sources 87 (2000) 28–38.
[16] H. Cordatos, T. Bunluesin, J. Stubenrauch, J.M. Vohs and R.J. Gorte, J. Phy. Chem. 100 (1996) 785.